Earth`s Cryosphere, 2018, vol. XXII, No. 4, pp. 75–83 **http://earthcryosphere.ru/**

DOI: 10.21782/EC2541-9994-2018-4(75-83)

APPLICATION OF HIGH-FREQUENCY GROUND PENETRATING RADAR TO INVESTIGATIONS OF PERMAFROST-AFFECTED SOILS OF PEAT PLATEAUS (EUROPEAN NORTHEAST OF RUSSIA)

D.A. Kaverin[1], A.V. Khilko[2], A.V. Pastukhov[1]

[1] *Institute of Biology, Komi Science Centre, 28, Kommunisticheskaya str., Syktyvkar, 167982, Russia*
[2] *Fundamentproject, 1/1, Volokolamskoe sh., Moscow, 125080, Russia; dkav@mail.ru*

Applications of high-frequency GPR to investigating permafrost-affected soils of peat plateaus have been analyzed. To assess the technical capabilities of high-frequency antennas, the depth of both permafrost table and lithological contacts at virgin (peat mounds and fens) and anthropogenically transformed (zone of defrosting influence of the cement-concrete road) sites of peat plateaus have been determined. The 300 and 900 MHz-frequency surface shielded antennas were used simultaneously in the conditions of considerable variability of the depth of permafrost table and mineral horizons bedding in the upper 10-meter soil strata. Application of the shielded air-coupled 1000 and 2000 MHz antennas to determining the permafrost table depth has been additionally assessed.

High frequency ground penetrating radar, permafrost, peat plateaus, road

INTRODUCTION

GPR investigations of soils, besides being a part of different scientific research, are widely used in various fields of engineering and geotechnical research [*Pyagay et al., 2009*]. GPR applications are equally much in demand in the studies of permafrost occurrence patterns in the cryolithozone [*Neradovskii, 2014; Tregubov et al., 2017*]. The methods for determining the depth of permafrost table are based on the contrast of electromagnetic properties of thawed and frozen horizons [*Frolov, 1998; Moorman et al., 2003*], which is one of primary concerns of the GPR surveying technique [*Wu et al., 2009; Gusmeroli et al., 2015*].

The study of permafrost table depth variability along with stratigraphic drilling is carried out using both low-frequency (100–200 MHz) [*Cao et al., 2017*] and high-frequency (300–400 MHz) antennas [*Bricheva and Krylov, 2014*]. The use of high-frequency antennas in GPR sounding allows a comprehensive analysis of the structure of the upper permafrost horizon taking into account the presently developing cryogenic phenomena and processes (frost heave, polygonal cracking, ice-wedge formation, etc.).

The geophysical methods employed in the study of permafrost-affected soil complexes [*Wollschläger et al., 2010; Abakumov and Tomashunas, 2016*] enabled determinations of both the permafrost table depth and organo-mineral interactions in the soil. GPR studies of permafrost-affected soils may be highly relevant for the studies of transitional layer (from peat deposits to the living vegetative cover) [*Shur et al., 2005*] and characterization of microtopography of the permafrost table [*Lupachev et al., 2016*]. However, the application of geophysical methods, specifically, GPR surveys, to the study of permafrost-affected soils is largely restrained due to thus far remaining unresolved problem of choosing optimal high-frequency range in the conditions of significant variability of the permafrost table occurrence depth.

This work aims to determine technical capabilities of the of GPR high- frequency sounding method to studying soils both at virgin (undisturbed) sites and anthropogenically transformed ones within the impact zone of the cement-concrete road (road-effect zone (REZ)) in permafrost areas occupied by peat plateaus. The features of the permafrost table topography and lithological boundaries (contacts) under highly variable conditions of their occurrence depth have been revealed and described by this research.

OBJECTS OF STUDY

The GPR surveying of soils was carried out along the three profiles delineating the permafrost peat plateaus, which are perpendicularly crossed by the Usinsk–Kharyaga highway (Fig. 1). Given its re-

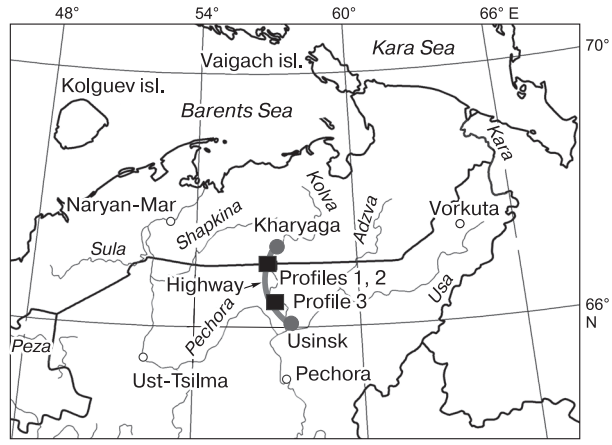

Fig. 1. Geographical position of the objects of study.

Table 1. **Characteristics of the objects of study**

Control-Point No. (CP)	Landscape	Plant community	Maximal height of vegetation storey, cm	Permafrost table depth, cm	Relative elevation of profile points, m
		Profile 1			
0	Flat top of peat mound	Dwarf birch-herbaceous-mossy	10	90	3
10	Upper part of flat-topped peat mound	Ledum-dwarf birch-lichen	30	40	3
20	Slope surface in the upper part of the slope of peat mound	Ledum-dwarf birch-lichen	30	47	3
30	Gently tilted surface of the slope of peat mound	Subshrub-dwarf birch-mossy-lichen	40	52	3
40	Middle part of the slope of peat mound	Willow shrub, herbaceous-dwarf birch	80	105	2
50	Roadside subsidence	Willow herbaceous-mossy	450	50	0
60	Roadside subsidence	Willow, herbaceous-mossy	400	>130	1
70	Base of road embankment (east-facing)	Willow, herbaceous-dwarf birch	80	>130	1
80	Shoulder (east-facing) of the road embankment	Sparse vegetative cover: willow herb, horsepine, herbs	50	>130	5
90	Shoulder (west-facing) of the road embankment	Sparse vegetative cover: willow herb, horsepine, herbs grasses	30	>130	5
100	Base of the road embankment (west-facing)	Willow shrub, herbaceous	200	>130	1
		Profile 2			
0	Summit of peat mound	Dwarf birch-subshrub-lichen	15	55	2
10	Middle part of the slope of peat mound	Dwarf birch-subshrub-mossy-lichen	40	36	1
20	Waterlogged roadside subsidence, hummocky relief	Willow, dwarf Arctic	120	>130	0
30	Waterlogged roadside subsidence with a ditch developed at the base of road embankment	Willow, dwarf Arctic	150	>130	0
40	Shoulder of the slope (east-facing) of road embankment (5 m in height; slope angle is c. 45°). The road infill is silty detrital sands	Barren	0	>130	5
50	Shoulder of the slope (west-facing) of road embankment (5 m in height; slope angle is c. 45°)	Barren	0	>130	5
60	Base of road embankment at the contact with waterlogged roadside subsidence	Willow, dwarf Arctic-herbaceous	130	>130	0
70	Gentle slope (base) of peat mound adjacent to roadside ditch	Willow-dwarf birch-subshrub-mossy	130	>130	1
80	Flat top of peat mound	Dwarf birch-subshrub-mossy-lichen	30	55	2
90	Flat top of peat mound	Dwarf birch-subshrub-mossy-lichen	30	42	2
100	Flat top of peat mound	Dwarf birch-subshrub mossy-lichen	30	44	2
110	Marginal drained part of peat mound	Lichen-mossy with subshrubs	20	58	2
120	Lower part of slope (flat base) of peat mound	Lichen-mossy-subshrub	30	40	1
130	Middle part of the slope of peat mound	Lichen-mossy-subshrub	20	58	2

gional status, the road is dominantly used to maintain operations of the oil industry's production facilities. The road length totals 164 km, with most of it paved with cement-concrete slabs. The northern segment of the highway runs in the permafrost zone.

Profiles 1 and 2 (Nenets Autonomous district) are spaced at a distance of 500 m (coordinates: 67°01′ N, 56°54′ E) within the southern tundra at the boundary between the forest tundra which belongs to the zone of non-continuous permafrost distribution [*Oberman and Shesler, 2009*]. Profile 3 (coordinates: 66°23′ N, 57°54′ E) (Fig. 1), is laid in the Usinsk region of the Komi Republic on a peat plateau in the northernmost taiga with sporadic island distribution of permafrost. Mean annual air temperature of the study area is –4 °C, mean annual precipitation is about 500 mm [*Fedorov, 1976*]. The fieldworks were carried out in August 2016.

The thickness of peat stratum varies from 3.5 m (Profiles 1 and 2), to about 1 m (Profile 3). Profiles 1 and 3 run along the "peat plateau – highway" transect, while Profile 2 is located on the "peat plateau – highway–peat plateau" transect. The undisturbed sites feature either the predominance of peat oligotrophic permafrost-affected soils (Profiles 1 and 2) or peat oligotrophic deep permafrost-affected soils (Profile 3). While roadside depressions and road embankments are characterized by embryozems. The study objects are described in detail in Table 1.

RESEARCH METHODS

The permafrost table depth was measured by GPR using "Zond-12E" systems (Radar Systems, Inc., Riga, Latvia) with shielded ground-coupled 300 and 900 MHz antennas and shielded air-coupled 1000 and 2000 MHz antennas. The application of antennas with different frequencies served the purpose of testing their relevancy for highly variable permafrost table depth and lithological contacts at both virgin and anthropogenically disturbed sites of peat plateaus.

Moreover, the use of different high-frequency antennas allowed to rule out technical interference caused by a complex terrain of the soil surface. The 300 and 900 MHz ground-coupled antennas moved directly along the soil surface attached to a compatible measuring wheel (125 mm in diameter), taking measurements with a rate of 128 pulses per revolution. The 1000 and 2000 MHz air-coupled antennas which do not require direct contact with the soil surface, were carried while walking at a height of 0.5 m and, allowing it moving directly over the soil surface along the profile line.

The GPR survey was conducted in a continuous mode, with an open data-link interface. Georeferencing was carried out by means of control points (CPs) of the profile with 10 m spacing (CP 10, 20, etc.). The values of reference (intermediate) points (CP 15, 28, etc.) were applicable in the processing and analysis of spatially differentiated GPR data. The CP number reflects the distance (in meters) at which the points stands out from the starting point of the profile (CP 0).

The obtained GPR data were processed in the Prizm 2.60.02 software package (Radar Systems, Inc., Riga, Latvia). The applied algorithms recommended by the manufacturer for the office processing of the obtained GPR data involve: removal of the "ringing" noise from the GPR data; bandpass filtering using a cosine filter; automatic gain adjustment; signal conversion from time to depth scale; the contribution of various topographic variables.

When converting the signal from time to depth scale, the average velocity of electromagnetic wave (v) was taken into account, which in the active layer (AL) is 10 cm/ns at soil permeability $\varepsilon'_r = 9$. For permafrost $v = 15$ cm/ns, $\varepsilon'_r = 4$, for water-mass (waterlogged areas) $v = 3.3$ cm/ns, $\varepsilon'_r = 81$.

The estimation of maximum resolution of vertical GPR sounding was calculated by the formula

$$\frac{1}{2}\lambda = \frac{v}{2f}, \quad (1)$$

где $\frac{1}{2}\lambda$ is vertical resolution of survey, equal to half the length of the electromagnetic (EM) wave; v is propagation velocity of EM wave; f is upper frequency of the signal.

The horizontal resolution limit was estimated from the radius of the effective reflecting area of the point source:

$$\frac{1}{2}\sqrt{\lambda h}, \quad (2)$$

where λ is wavelength; h is the depth of the target horizon.

Analysis of the signal amplitude spectra ranges of different antennas coupled with the formulas (1), (2) [*Boganik and Gurvich, 2006*] allowed estimating maximal vertical and horizontal resolution of the deployed high-frequency antennas (Table 2). The control points of the profiles were used for: identifying the landscape components and vegetation types; measuring relative elevations of the points with the Geobox N8-32 optical level; measuring the permafrost table depth with graduated metal probe (length: 130 cm). For morphology determinations on soil (0–1 m depth interval) and underlying rocks (1–10 m) of Profiles 1 and 2, soil sections were cut out on the peat plateau surface and at the base of road embankment, complemented by drilling soil wells No. 1 and 2, with subsequent sampling. Given a thin peat layer (about 1 m) along Profile 3, soil well No. 3 was drilled to a depth of 1.5 m. The permafrost table

Table 2. **Horizontal and vertical resolution characteristics of the applied high-frequency antennas**

Depth, m	Antenna frequency, MHz							
	300		900		1000		2000	
	AL	Permafrost	AL	Permafrost	AL	Permafrost	AL	Permafrost
	Horizontal resolution, cm							
1	37	45	24	30	15	19	16	20
2	52	63	34	42	22	26	23	28
3	63	77	42	51	–	–	–	–
4	73	89	48	59	–	–	–	–
5	82	100	54	66	–	–	–	–
6	89	109	–	–	–	–	–	–
7	96	118	–	–	–	–	–	–
	Vertical resolution, cm							
	27	40	12	18	5	7	6	8

Note. Dash means the absence of measuments. AL – active layer.

depth measurements, along with the drill core and soil sections data were cumulatively used as reference data for determining spatial variations of the permafrost table topography and of the lower boundaries of peat and technogenic (infill) horizons.

RESEARCH RESULTS

The results of GPR sounding using the 300 MHz antenna have exhibited a distinctly discernible "equal phase line" (reflection) on GPR profile 1 (CP 0-71 segment), associated with a reflection from the permafrost table (Fig. 2). In the case of virgin peat massif, the permafrost depth varies in the range from 0.2 to 1.5 m, while the AL thickness (ALT) is tending to increase on the slope of the peat mound adjacent to highway (CP 40). A gently dipping permafrost table (from the depth of 1 to 2 m) in the direction of the road embankment base is reported within the CP 60–70 profile points interval.

The permafrost table position can be traced quite clearly on the GPR section of Profile 2 (Fig. 3). The

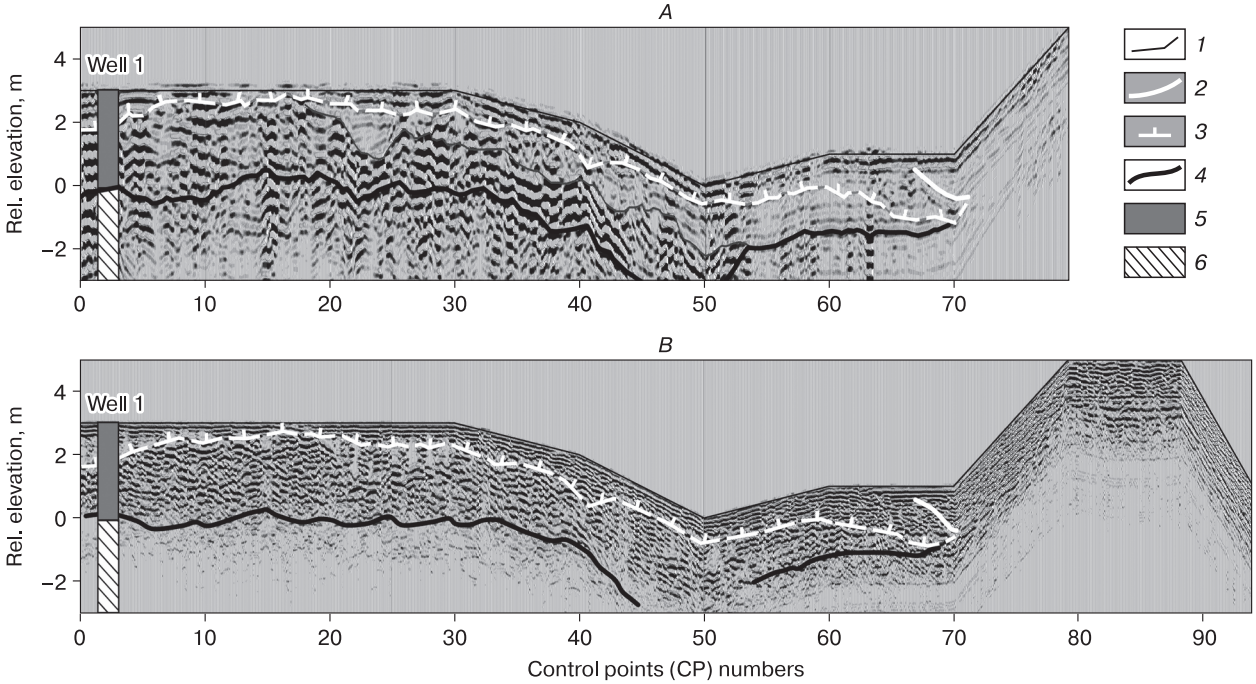

Fig. 2. GPR section along Profile 1 resulting from the radar survey using the 300 MHz (*A*) and 900 MHz (*B*) antennas.

1 – generalized soil surface topography; *2* – base of technogenic infill soils; *3* – permafrost table; *4* – lower limit of peat horizons; *5* – peat soils; *6* – silty clay-loams.

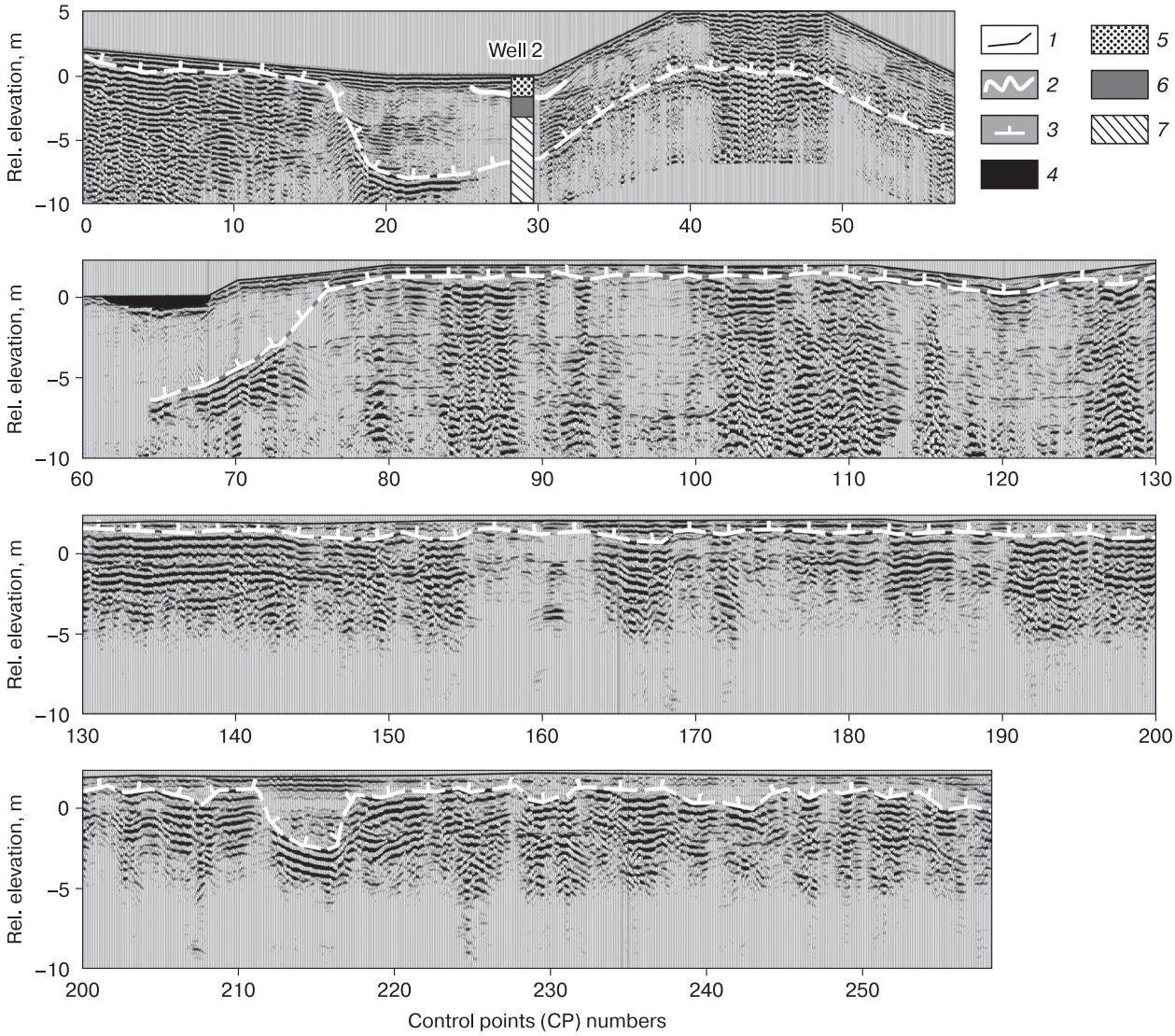

Fig. 3. GPR section along Profile 2 resulting from radar survey using the 300 MHz antenna.

1 – generalized soil surface topography; *2* – base of technogenic infill soils; *3* – permafrost table; *4* – water in roadside ditch; *5* – infill sand-loam – gravel soils; *6* – peat soils; *7* – silty clay-loams.

boundary delineates the reflection separating the areas with different types of signal recording. In regions where the signal record boundary position is nearly vertical, it is manifested as a series of diffraction wavefronts. At the profile's start point (0–15 CPs) the permafrost table depth ranges from 0.5 to 0.9 m in the peat plateau, nearly plummeting down within the roadside subsidence from 1 m (CP 17) to 8 m (CP 21). Further, the permafrost table gradually rises to the level of 6.5 m beneath the road embankment base (CP 30) and to 4–5 m (CP 40) beneath the embankment (CP 40–60) (Fig. 3). Within the roadside subsidence area in western part of the profile, the permafrost table shows yet another declining trend lowering down to a depth of 5.0–6.5 m (CP 64–70). A relative stabilization of permafrost occurrence depth (0.5–1.0 m) is observed on the slope of the peat mound adjacent to roadside subsidence (CP 75–90) (Fig. 3). Locally, beneath the fens (3–4 m in diameter) the permafrost table occurs within the 1–2 m depth interval (CP 164–169; 205–208; 227–231). The maximum lowering of the permafrost table to 4.5 m is reported under the largest fen, 7–9 m in diameter (CP 211–218) (Fig. 3).

GPR sounding of virgin soils of the peat plateau along Profile 3 revealed a relatively deep (1.5–2.0 m) occurrence of permafrost table depth (Fig. 4). Directly under the base of the slope of the road embankment (height: 2 m), the permafrost table is lowered to a depth of 2.5 m.

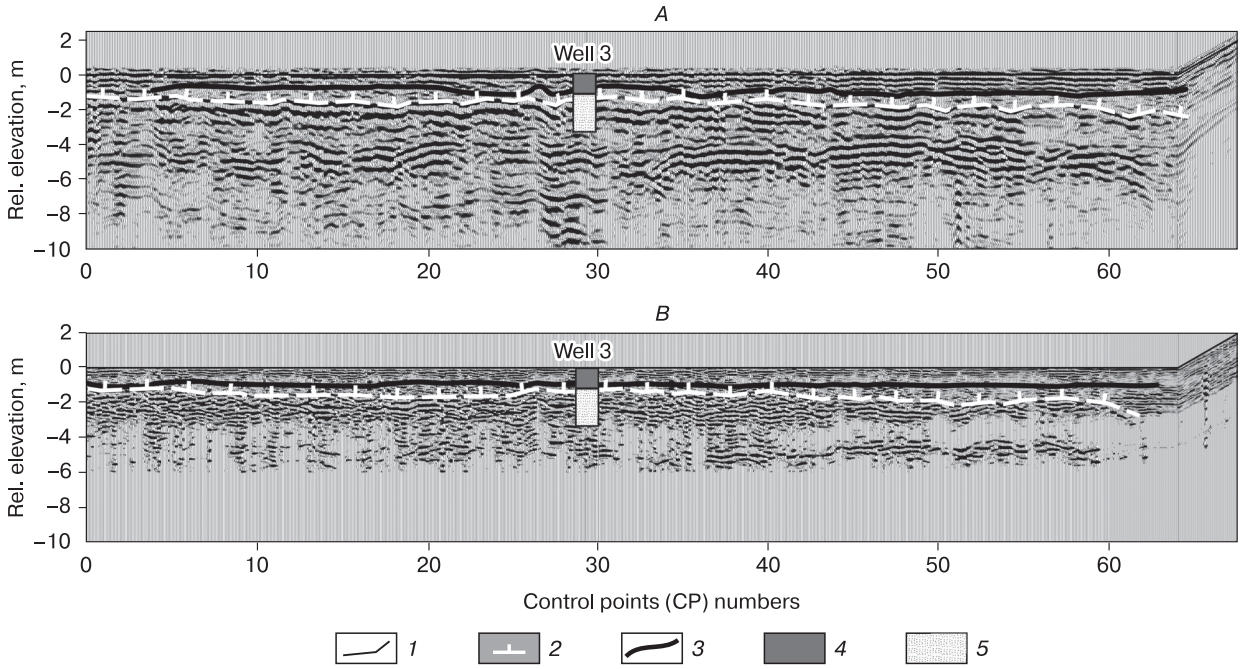

Fig. 4. GPR section along Profile 3 resulting from radar survey using the 300 MHz (*A*) and 900 MHz (*B*) antennas.

1 – generalized soil surface topography; *2* – permafrost table; *3* – lower limit of peat horizons; *4* – peat soils; *5* – sands.

The GPR data analysis for Profile 1 allows distinguishing lower limits of peat horizons and technogenic (infill) soils (Fig. 2). The thickness of the latter increases from 0.5 to 1.6 m (CP 67–70) towards the base of the road embankment. The reflection corresponding to the lower limit of peat horizons can be traced almost throughout the whole profile at a depth from 2.2 to 4.0 m. At this, the maximum thickness of the peat layer base is reported in the marginal part of the peat mound bordering the roadside subsidence (CP 45–50). Beneath the road embankment, the lower limit of peat layer occurs at a depth of 3 m, which indicates that the road infill rest immediately on the peatland layer. The Profile 2 sounding data also allowed identifying the lower limit of technogenic (infill) soils in the road embankment base (CP 25–31) at a depth of 1.0–1.7 m (Fig. 3). In the section along Profile 3, the lower limit of a thin peat layer is distinctly observed within the 0.6–1.2 m depth interval (CP 4–64) (Fig. 4).

Analysis of results of the GPR surveys using 900 MHz antenna allows tracing and specifying the occurrence pattern of both permafrost table and other lithological elements along the profile (Fig. 2, 4, 5). However, permafrost table occurring deeper than 2 m can be traced not as clearly as when the GPR surveys using 300 MHz antenna is applied. At these depths, continuous tracing of the reflection corresponding to this and other boundaries on the profile appears impossible. Thus, the lower boundary of the peat layer is still relatively discernible in the changing wave pattern of Profile 1 (CP 0–44). However, in the underlying loamy horizons the record becomes more elusive (Fig. 2).

With GPR sounding using the shielded air-coupled 1000 and 2000 MHz antennas, the depth of clearly displayed signal constituted 0.3 m, which is utterly insufficient for determinations of the depth of permafrost table and lithological contacts (Fig. 6).

DISCUSSION OF RESULTS

The use of shielded antennas with different frequencies allowed studying their performance features, advantages and disadvantages of their application to determining the depth of permafrost table and lithological contacts both in virgin and anthropogenically disturbed areas of peat plateaus. The 300 MHz-frequency antenna which penetrates to a greater depth can provide for measurements of the permafrost occurrence depth and lithological contacts within the upper 10-meter subsurface. The penetrating capacity of the 300 MHz antenna is sufficient to detect changes in the permafrost table occurrence depth in a wide interval (0–10 m) allowing to detect the lower boundary of deep taliks beneath the lakes and in the road effect zone. While higher resolution of the 900 MHz antenna enables greater detail of the topography of permafrost and lithological contacts in the 0–2 m depth interval. However, lower penetra-

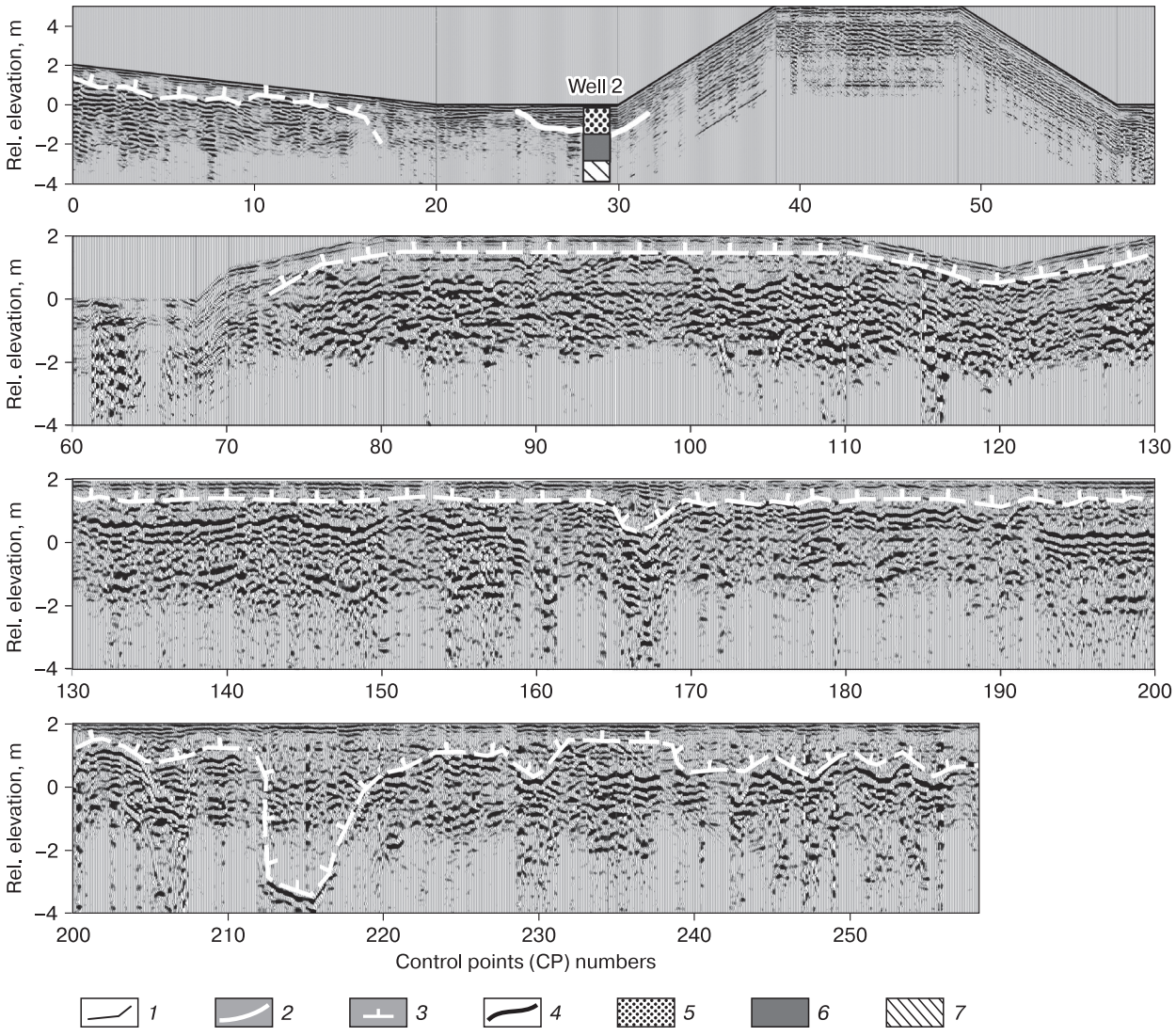

Fig. 5. GPR section along Profile 2 resulting from radar survey using the 900 MHz antenna.

1 – generalized soil surface topography; *2* – base of technogenic infill soils; *3* – permafrost table; *4* – lower limit of peat horizons; *5* – infill sand-loam – gravel soils; *6* – peat soils; *7* – silty clay-loams.

tion of the radio signal of this antenna limits its capabilities when sounding the deepened permafrost table (to a depth of 2–8 m). Thus, the 900 MHz antenna can be used in the conditions of predominantly shallow occurrence of permafrost table, in the absence of deep talik zones. Using it is more appropriate for a detailed study of undisturbed permafrost-affected soil complexes.

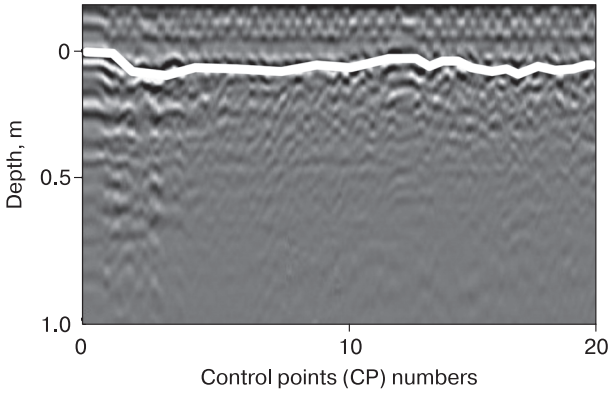

Fig. 6. GPR section of the fragment of Profile 1 resulting from radar survey using the 1000 MHz antenna (without account of relief data input).

White line indicates reflection from the soil surface.

As follows from the results of GPR surveys using 1000 and 2000 MHz antennas, that these have insufficient depth of signal penetration and are found uninformative with respect to determining the permafrost table configuration in the tundra soils. Instead, high-frequency air coupled shielded antennas are more suitable for sounding roads, bridges, brick and concrete structures [*Radar... systems, 2017*].

Analysis of the research results has shown that the road warming effect zone can be traced to a distance of up to 15 m from the base of the embankment slope (Fig. 2–4). The total width of REZ in the areas of permafrost-underlain peat plateaus can thus reach 50 m. The most appreciable decrease in the permafrost table (up to 6–8 m) is observed under roadside subsidences, which create favorable conditions for waterlogging and for growth of higher-shrub vegetation, as well as for snow accumulation (Table 1). This, in turn, leads to an increase in winter soil temperatures, causing thereby thaw of ice-rich horizons. A relative elevation of the permafrost table to the level of 5–6 m beneath the road embankment can be accounted for a thin indurated snow layer forming annually on the road surface during its winter-time operations. Given the sporadic-island pattern of the underlying permafrost, the road with a relatively low embankment (2 m) crossing the peat plateau causes a 20–40 % increase in the permafrost table occurrence depth. In this case, the warming impact of the road expands only to a distance of 5 m down from the base of slope of the road embankment.

More detailed characterization of the thermal regime of the roadside subsidence zone will be discussed in the paper with a focus on changes in the temperature state of soils during the year-round road operation.

CONCLUSIONS

The use of modern high-frequency GPR technologies allows investigating the spatial differentiation of the depth of both permafrost table and lithological contacts in virgin and anthropogenically disturbed soils of peat plateaus.

The combined use of 300 and 900 MHz-frequency ground-coupled shielded antennas is an effective solution for determining significant variations (0–10 m) in the depth of permafrost table and lithological contacts (the lower limit of peat layer and technogenic soils). Higher penetration of the 300 MHz antenna signal broadens the scope of investigation of the configuration of deep closed taliks (2–8 m) within the road warming impact zone and beneath the fens. While high frequency antenna (900 MHz) allows studying in detail the permafrost table topography in the 0–2 m depth strata, which is critical in the investigations of virgin permafrost-affected soil complexes.

The low penetration of high-frequency (1000 and 2000 MHz) air-coupled shielded antennas has proven them inadequate for the research of soils of permafrost peat plateaus. The results of high-frequency GPR surveys revealed that the construction and operation of a cement-concrete highway running across peat plateaus in the southern parts of the permafrost zone contributes to a significant lowering of the permafrost table (up to 8 m).

The warming (defrosting) effect of the road is significant in the zone up to 50 m in width, comprising the road embankment, roadside depressions and adjacent areas of peat plateaus. The virgin sites of peat plateaus are characterized by heterogeneity of permafrost table occurrence caused by the mesotopography of peat mounds and fens.

The research was supported by the project No. 141y 2016 within the framework of the UNDP/GEF project 00059042 with the financial support from the Russian Foundation for Basic Research (projects No. 18-55-11003; 18-05-60005; 16-04-00749).

References

Abakumov, E., Tomashunas, V., 2016. Electric resistivity of soils and upper permafrost layer of the Gydan Peninsula. Polarforschung, No. 86 (1), p. 27–34.

Boganik, G.N., Gurvich, I.I., 2006. Seismic Exploration. AIS, Tver, 744 pp. (in Russian)

Bricheva, S.S., Krylov, S.S., 2014. GPR investigations of near-surface permafrost soils on the Gydan peninsula. Inzh. Isyskaniya, No. 9–10, 38–44.

Cao, B., Gruber, S., Zhang, T., et al., 2017. Spatial variability of active layer thickness detected by ground-penetrating radar in the Qilian Mountains, Western China. J. Geophys. Res. Earth Surf., No. 122, 574–591, DOI: 10.1002/2016JF004018.

Fedorov, D.F. (Ed.), 1976. Atlas of Arkhangelsk Region. GUGK, Moscow, 72 pp. (in Russian)

Frolov, A.D., 1998. Electrical and elastic properties of frozen rocks and ice. ONTI PNTs RAN, Pushchino, 515 pp. (in Russian)

Gusmeroli, A., Liu, L., Schaefer, K., et al., 2015. Active layer stratigraphy and organic layer thickness at a thermokarst site in Arctic Alaska identified using ground penetrating radar. Arctic, Antarctic, and Alpine Res., No. 47 (2), 195–202, DOI: 10.1657/AAAR00C-13-301.

Lupachev, A.V., Gubin, S.V., Veremeeva, A.A., Kaverin, D.A., Pastukhov, A.V., Yakimov, A.S., 2016. Microrelief of the permafrost table: structure and ecological functions. Earth's Cryosphere XX (2), 3–13.

Moorman, B.J., Robinson, S.D., Burgess, M.M., 2003. Imaging periglacial conditions with ground-penetrating radar. Permafrost and Periglacial Processes, No. 14, 19–329, DOI: 10.1002/ppp.463.

Neradovskii, L.G., 2014. Estimating the Thermal State of Permafrost by Electromagnetic Sounding Methods. ANO "Nauchnoe obosrenie" Publishing House, Moscow, 333 pp. (in Russian)

Oberman, N.G., Shesler, I.G., 2009. Observed and projected changes in permafrost conditions within the European

Northeast of Russia. Problemy Severa i Arktiki RF. Nauchn.-inform. Byul., iss. 9, 96–106.

Pyagay, E.T., Belobrov, V.P., Molchanov, E.N., Seo, M.Ch., Son, Y.K., 2009. Application of GPR in soil studies. Byul. Pochv. In-ta, No. 64, 106–125.

Radar and Seismic systems. 1.0 GHz aerial antenna, shielded [Electronic resource]. – URL: http://radseismsys.ru/catalog/antenny/antenna-1-0-ggts-vozdushnaya-ekranirovannaya (submittal date: 16.06.2017).

Shur, Y., Hinkel, K.M., Nelson, F.E., 2005. The transient layer: implications for geocryology and climate-change science. Permafrost and Periglacial Processes, No. 16, 5–17, DOI: 10.1002/ppp.518.

Tregubov, O.D., Kraev, G.N., Maslakov, A.A., 2017. Modelling the permafrost table structure from the GPR survey data. Extended abstract submitted to EAGE Conference and Exhibition Engineering Geophysics on April 24–28 2017, Kislovodsk, Russia, DOI: 10.3997/2214-4609.201700389.

Wollschläger, U., Gerhards, H., Yu, Q., Roth, K., 2010. Multichannel ground-penetrating radar to explore spatial variations in thaw depth and moisture content in the active layer of a permafrost site. The Cryosphere, No. 4, 269–283, DOI: 10.5194/tc-4-269-2010.

Wu, T., Wang, Q., Watanabe, M., et al., 2009. Mapping vertical profile of discontinuous permafrost with ground penetrating radar at Nalaikh depression, Mongolia. Environ. Geology, No. 56, 1577–1583, DOI: 10.1007/s00254-008-1255-7.

Received June 22, 2017